Thermodynamic Behavior of the $CO_2 + NO_2/N_2O_4$ Mixture: A Monte Carlo Simulation Study

Emeric Bourasseau,*,† Veronique Lachet,‡ Nicolas Desbiens,† Jean-Bernard Maillet,† Jean-Marie Teuler,§ and Philippe Ungerer||

Commissariat à l'Energie Atomique, Centre DAM−Ile de France, Département de Physique Théorique et Appliquée, Bruyères-le-Châtel, 91297 Arpajon Cedex, France, IFP, Direction Chimie et Physico-Chimie Appliquées, 1-4 Avenue du bois Préau, 92852 Rueil-Malmaison Cedex, France, IFP, Direction Scientifique, 1-4 Avenue du bois Préau, 92852 Rueil-Malmaison Cedex, France, and Université de Paris Sud, Laboratoire de Chimie Physique, UMR CNRS 8000, 91405 Orsay, France

Received: July 31, 2008; Revised Manuscript Received: September 25, 2008

The thermodynamic behavior of the carbon dioxide + nitrogen dioxide ($CO_2 + NO_2$) mixture was investigated using a Monte Carlo molecular simulation approach. This system is a particularly challenging one because nitrogen dioxide exists as a mixture of monomers (NO_2) and dimers (N_2O_4) under certain pressure and temperature conditions. The chemical equilibrium between N_2O_4 and $2NO_2$ and the vapor−liquid equilibrium of $CO_2 + NO_2/N_2O_4$ mixtures were simulated using simultaneously the reaction ensemble and the Gibbs ensemble Monte Carlo (RxMC and GEMC) methods. Rigid all atoms molecular potentials bearing point charges were proposed to model both NO_2 and N_2O_4 species. Liquid−vapor coexistence properties of the reacting NO_2/N_2O_4 system were first investigated. The calculated vapor pressures and coexisting densities were compared to experimental values, leading to an average deviation of 10% for vapor pressures and 6% for liquid densities. The critical region was also addressed successfully using the subcritical Monte Carlo simulation results and some appropriate scaling laws. Predictions of $CO_2 + NO_2/N_2O_4$ phase diagrams at 300, 313, and 330 K were then proposed. Derivative properties calculations were also performed in the reaction ensemble at constant pressure and temperature for both NO_2/N_2O_4 and $CO_2 + NO_2/N_2O_4$ systems. The calculated heat capacities show a maximum in the temperature range where N_2O_4 dissociation occurs, in agreement with available experimental data.

Introduction

The risks associated with climate change have been the subject of much debate in recent years. Nowadays, most experts think that these risks are real and directly linked to the increase of the emission of greenhouse gases, especially CO_2. Among the various options for mitigating these emissions, large-scale CO_2 capture and storage into underground formations like deep saline aquifers or depleted oil and gas fields is a promising option.[1] One economical and energetic limitation of such capture and storage operations might be the required purity of the CO_2 stream.[2] The quality of the CO_2 captured from power plants or industrial installations depends on several factors, like the nature of the fossil combustible involved, the processes used for combustion and capture, and the possible use of further treatments. Depending on these factors, the CO_2 stream will account for a variable amount of gas contaminants, such as SO_2, NO_x, H_2S, N_2, O_2, Ar, etc., that can reach up to a few mole percent. A detailed inventory of the nature and concentration of contaminants has been proposed by Anheden et al. in 2004.[3] However, only few studies have investigated till now the impact of these contaminants on capture, transportation, injection, and storage operations. It is thus not yet possible to define precise maximal amounts of contaminants that can be tolerated in CO_2 flues. Accurate knowledge of the thermodynamic behavior of CO_2−contaminant mixtures is part of the required studies in order to address the impact of these contaminants and to develop optimized carbon dioxide capture and storage solutions.

Some of these CO_2−contaminant mixtures, like CO_2-O_2 and CO_2-N_2 for instance, have been already studied over a large range of pressures and temperatures. In the case of CO_2-SO_2 and CO_2-NO_2 mixtures, thermodynamic data are very scarce or nonexistent. To the best of our knowledge, the recent work of Belkadi and co-workers[4] using the soft-SAFT equation of state is the only study devoted to the thermodynamic behavior of the CO_2-NO_2 mixture. This system is a particularly challenging one because nitrogen dioxide exists as a mixture of monomers (NO_2: nitrogen dioxide) and dimers (N_2O_4: dinitrogen tetroxide). The composition of the $NO_2-N_2O_4$ equilibrium mixture depends on pressure and temperature conditions: the dimer is favored at higher pressures and lower temperatures. Without CO_2, the chemical equilibrium between N_2O_4 and $2NO_2$ has been the subject of some experimental work[5−10] and of some theoretical investigations.[11−13] In the liquid and solid states, this reaction has been studied by James and Marshall[10] who measured equilibrium constants from 77 to 295 K. From this study, it can be inferred that nitrogen dioxide is strongly associated in the liquid phase, leading to some dimerization fractions of more than 0.99 at temperatures lying between 250 and 295 K. In the gas phase, dimerization can also occur but the fraction of associated molecules (N_2O_4) rapidly decreases as the temperature increases or the pressure decreases, following Le Chatelier's principle for endothermic

* Corresponding author. E-mail: emeric.bourasseau@cea.fr.
† Département de Physique Théorique et Appliquée.
‡ IFP, Direction Chimie et Physico-Chimie Appliquées.
§ Université de Paris Sud.
|| IFP, Direction Scientifique.

10.1021/jp8068255 CCC: $40.75
Published on Web 11/14/2008

dissociation reactions. Chao and co-workers[11] have reported values of standard Gibbs energy change ΔG_r° (298.15 K) and standard enthalpy change ΔH_r° (298.15 K) reaction of 1.138 and 13.67 kcal·mol^{-1}, respectively. Equilibrium constants of the reaction in the gas phase have been studied by several authors: Yoshino,[6] Verhoek,[7] and Harris,[8] among others. Reported values show a molar composition of the vapor phase around 90 mol % of NO_2 at 373.15 K and a complete dissociation into NO_2 at 413.15 K. Concerning its kinetics, the dissociation reaction $N_2O_4 \rightarrow 2NO_2$ is very fast, with some rate constants reported by Cher[9] of $1.7 \times 10^5 - 1.0 \times 10^6$ s^{-1} at room temperature. In addition to these studies of the $N_2O_4 \rightleftarrows 2NO_2$ chemical equilibrium, phase behaviours and phase properties of the $NO_2-N_2O_4$ reacting system have also been investigated in the literature from experimental studies[14−16] or from empirical modeling approaches.[17] Reamer and Sage[14] have reported vapor pressures and density measurements in the liquid−vapor coexistence region, as well as liquid densities in the one-phase region. Low temperature liquid densities are available from the work of Gray et al.,[15] and McCollum[18] has reported some values of heat capacities of this reacting system at atmospheric pressure.

In this work, the chemical equilibrium between N_2O_4 and $2NO_2$ as well as the vapor−liquid equilibrium of $CO_2 + NO_2/N_2O_4$ mixtures were simulated at a molecular level using simultaneously the reaction ensemble and the Gibbs ensemble Monte Carlo methods. The reaction ensemble Monte Carlo method (RxMC)[19,20] allows the study of chemically reacting mixtures using the so-called reaction move in order to fulfill reaction equilibrium criteria (see ref 21 for a recent review of applications), whereas the Gibbs ensemble Monte Carlo method (GEMC)[22] enables the calculation of phase equilibrium by introducing some separate simulation boxes that can exchange molecules. Both methods are using standard molecular potentials. Only a few attempts have been already done to combine the RxMC and the GEMC methods: Lisal and co-workers have studied vapor−liquid equilibria of the reacting $Br_2 + Cl_2 +$ BrCl mixture[23] and vapor−liquid equilibria of reacting MTBE system.[24] The combination of the RxMC and GEMC methods is used here in order to study the NO_2/N_2O_4 and the $CO_2 + NO_2/N_2O_4$ systems at both chemical and phase equilibrium. Such simulations have been performed either at constant total volume and constant temperature or at constant pressure and constant temperature. In this study, standard rigid All Atoms molecular potentials bearing point charges were used to model NO_2, N_2O_4, and CO_2 molecules. In case of NO_2 and N_2O_4 potentials, 12-6 Lennard-Jones parameters have been fitted to reproduce experimental data of Reamer and Sage cited above.[14]

This paper is organized as follows. Simulation methods are described in section II, including the presentation of the fluctuation formula used to calculate derivative properties in the reaction ensemble. Molecular models developed for the study of NO_2 and N_2O_4 molecules are described in section II.C along with all simulation details. Results obtained for the $NO_2-N_2O_4$ system are discussed in section III.A, whereas section III.B is devoted to the results obtained for the $CO_2 + NO_2/N_2O_4$ mixture. Finally, section IV gives our conclusions.

II. Methods

A. RxMC Method. The goal of the RxMC method is to compute thermodynamic properties of a multi component system at chemical equilibrium. In order to fulfill the chemical equilibrium condition, a particular statistical ensemble is defined: the reaction ensemble. The complete definition of this ensemble as well as a rigorous derivation of its density probability have been done first by Smith and Triska.[19] Johnson has also given a very nice derivation of the reaction ensemble acceptance probability in ref 25. Here, we will only give a brief description of this ensemble and we invite interested readers to refer to those papers and our previous works[26,27] for more details. It is also interesting to consider the pioneer work of Shaw, who proposed earlier a method similar in nature to simulate chemical equilibrium of molecular mixtures.[28,29]

In this work, we are interested in using the RxMC method simultaneously with the Gibbs ensemble to compute a system at chemical and phase equilibrium. To preserve the internal equilibrium of the system, the following usual Monte Carlo moves are used: translation and rotation of molecules. To obtain the phase equilibria, the system is separated in two simulation boxes, and transfer moves between the two phases are applied. The system is simulated either at constant total volume or constant pressure. To ensure mechanical equilibrium of the system, the volume of each phase is modified using standard Monte Carlo volume changes. As a consequence, the simulations performed in this work are $N_{atoms}VT$ or $N_{atoms}PT$ RxMC GEMC simulations.

Here is given a brief description of the RxMC method. In comparison with the canonical ensemble, two additional constraints are applied in order to satisfy the chemical equilibrium condition:

• The number of atoms is fixed for each atom type, so the number of different molecules in the system is controlled by the chemical equation which defines the chemical equilibrium:

$$\sum_{i=1}^{s} \nu_i a_i = 0 \tag{2.1}$$

where ν_i is the stoichiometric coefficient of chemical species i. For example,

$$2NO_2 \rightleftarrows N_2O_4 \tag{2.2}$$

• The sum of chemical potentials μ_i over the different molecular species implied in the chemical reaction, weighted by stoichiometric coefficients, is equal to zero:

$$\sum_{i=1}^{s} \nu_i \mu_i = 0 \tag{2.3}$$

For exemple,

$$2\mu_{NO_2} = \mu_{N_2O_4} \tag{2.4}$$

The key point is to establish a Metropolis algorithm that satisfies these constraints during the simulation. In order to obtain the chemical equilibrium, an additional move is used: the so-called reaction move, proposed at the same time by Smith et al.[19] and Johnson et al.[20] This move consists first in choosing a direction to perform the reaction, second in deleting a set of reactant molecules randomly chosen in the system, and finally inserting product molecules. In our example, the reaction move is

$$2NO_2 \rightarrow N_2O_4 \tag{2.5}$$

where two randomly chosen NO_2 molecules are deleted and one N_2O_4 is inserted or

$$N_2O_4 \rightarrow 2NO_2 \tag{2.6}$$

where one N_2O_4 molecule randomly selected is deleted and two NO_2 molecules are inserted.

During this move, not only the energy is modified, but also the number of molecules of each species involved in the reaction. Introducing the parameter ξ, equal to 1 (respectively, -1) if the reaction move is performed in the forward (respectively, backward) direction, it is possible to establish the following acceptance probability:

$$P_{acc} = \min\left(1, (P_0\beta V)^{\xi\bar{\nu}} \exp\left(-\xi\frac{\Delta_r G^0(T)}{RT}\right) \times \prod_{i=1}^{s} \frac{N_i!}{(N_i + \xi\nu_i)!} \exp(-\beta\Delta U_{ext})\right) \tag{2.7}$$

where P_0 is the standard pressure, V is the volume, $\bar{\nu}$ is the stoichiometric coefficient sum, $\Delta_r G^0(T)$ is the standard free enthalpy of reaction at temperature T, N_i is the number of molecules of species i, and ΔU_{ext} is the intermolecular configurational energy difference of the system between states before and after the move.

Practically, the following algorithm is used to account for a reaction move:

- The direction of the move is randomly chosen ($\xi = -1$ or 1). This determines the type of the molecules of reactant to be deleted and the product molecules to be inserted.
- ν_i molecules of each reactant type are randomly chosen and deleted from the configuration.
- ν_j molecules of each product type are randomly inserted in the configuration (i.e., the place of insertion is randomly chosen).
- The energy of the *new* configuration is calculated, and the acceptance probability of the move is obtained using eq 2.7.
- According to the Metropolis algorithm, the new configuration is accepted or rejected in the Markovian chain depending on the comparison between the value of P_{acc} with a real randomly taken between 0 and 1.

Combining translation, rotation, and reaction moves, it is possible to simulate a chemical equilibrium for a given temperature and volume. Nevertheless, efficiency of the RxMC deteriorates with increasing density of the system. This limitation can be overcome using statistical biases in the algorithm that enhance the insertion probability. In this work, we used the preinsertion bias,[30] already implemented in our MC code. This bias applied to a reaction move consists first of all in inserting the first product molecules in the empty space left by the deleted reactant molecules. If the move is performed in the direction which products two NO_2 molecules, the second one is inserted at a preselected location using the following criterium: for each insertion, a set of k locations are tested with a simplified potential, and one position x is selected following the acceptance criterion detailed in reference.[30] Moreover, for each product molecule, a set of k' orientations are also tested. One orientation is then selected following the acceptance criterion detailed in ref 30. The acceptance probability of the reaction move then slightly differs from eq 2.7. The exact expression can be found in ref 26.

B. Fluctuation Formula in the Reaction Ensemble. In a previous work,[26] we have shown that starting from the reaction ensemble partition function defined by Smith,[19] it is possible to derive a fluctuation formulas which can be used to compute thermodynamic derivative properties:

$$\left(\frac{\partial\langle X\rangle}{\partial\beta}\right)_P = (\langle X\rangle\langle\hat{H}\rangle - \langle X\hat{H}\rangle) - \frac{1}{\beta}(\langle X\rangle\langle N_{tot}\rangle - \langle XN_{tot}\rangle) + \left(\langle X\rangle\left\langle\sum_{i=1}^{s}\frac{N_i}{\mathcal{N}_A}\Delta_f H_i^\circ(T)\right\rangle - \left\langle X\sum_{i=1}^{s}\frac{N_i}{\mathcal{N}_A}\Delta_f H_i^\circ(T)\right\rangle\right) \tag{2.8}$$

where X is a given property, N_i is the number of molecules of type i for a given state, $\hat{H}$ is the configurational enthalpy, ($\hat{H} = U^{ext} + U^{int} + PV$), $N_{tot} = \sum_i{}^s{}_{=1} N_i$ is the total number of molecules allowed to fluctuate during the simulation, and $\Delta_f H_i^\circ(T)$ is the standard enthalpy of formation of molecular type i at temperature T.

In fact, in comparison with the fluctuation formulas obtained in the isobaric−isothermal ensemble,[31] eq 2.8 takes into account not only the fluctuations of energy, but also the fluctuations of composition and number of molecules. From this equation, taking $X = V$, the coefficient of thermal expansion α_P can be calculated:

$$\alpha_P = \frac{1}{\langle V\rangle}\left(\frac{\partial\langle V\rangle}{\partial T}\right)_P \tag{2.9}$$

The derivation of heat capacity is more complicated. Indeed, it needs the derivation of the total energy with respect to temperature, including kinetic and internal potential energies. However, the kinetic energy K is not taken into account in a Monte Carlo simulation. In our calculations, the internal potential energy U^{int} is neither considered because of the use of rigid molecules. As a consequence, only the contributions arising from the derivative of the intermolecular energy U^{ext}, the derivative of the volume V, and the derivative of the number of molecules N_i can be calculated during the simulation. Other contributions, arising from the partition function of the isolated molecule, must be taken from ideal gas data available in thermodynamics compilations. The following decomposition of the total heat capacity is thus proposed:

$$C_P(T,P) = C_P^{int}(T,P) + C_P^{ext}(T,P) \tag{2.10}$$

with

$$C_P^{int}(T,P) = \left(\frac{\partial\langle H^{int}\rangle}{\partial T}\right)_{P,N_{atoms}} \tag{2.11}$$

and

$$C_P^{ext}(T,P) = \left(\frac{\partial\langle H^{ext}\rangle}{\partial T}\right)_{P,N_{atoms}} \tag{2.12}$$

where

$$H^{int} = U^{int} + K + NkT = \sum_i N_i\frac{\Delta_f H_i^\circ}{\mathcal{N}_A} \tag{2.13}$$

and

$$H^{\text{ext}} = U^{\text{ext}} + PV + NkT \tag{2.14}$$

The following operational expression can then be used:

$$C_P(T,P) = \sum_i \langle N_i \rangle C_{P_i}^{\circ}(T) + \sum_i \frac{\Delta_f H_i^{\circ}(T)}{\mathcal{N}_A}\left(\frac{\partial \langle N_i \rangle}{\partial T}\right)_{P,N_{\text{atoms}}} + \left(\frac{\partial \langle H^{\text{ext}} \rangle}{\partial T}\right)_{P,N_{\text{atoms}}} \tag{2.15}$$

In eq 2.15, the derivatives with respect to the temperature are calculated using eq 2.8 with $X = H^{\text{ext}}$ and $X = N_i$, whereas the ideal gas heat capacity $C_{P_i}^{\circ}$ and the standard formation enthalpy $\Delta_f H_i^{\circ}$ of species i are taken from thermodynamics tables. The proposed decomposition is analogous to the one proposed by Lagache and co-workers in the case of nonreacting systems,[31] except that the internal contribution is not an ideal property since it now depends on pressure, due to the pressure dependence of the composition.

In order to obtain the other derivative properties of interest, it is necessary to calculate the isothermal compressibility β_T whose expression is the same as in the isothermal−isobaric ensemble:

$$\beta_T = -\frac{1}{\langle V \rangle}\left(\frac{\partial \langle V \rangle}{\partial P}\right)_T = \frac{1}{\langle V \rangle kT}(\langle V^2 \rangle - \langle V \rangle^2) \tag{2.16}$$

The heat capacity at constant volume C_V can then be computed as:

$$C_V = C_P - \frac{\alpha_P{}^2 VT}{\beta_T} \tag{2.17}$$

It is important to note that the quantity X (for example $C_P(T,P)$) is extensive. To obtain the exact molar quantity, it is necessary to derive the molar quantity of X (for example the molar enthalpies h^{id} and h^{res}), introducing again the N_i's in the derivative, for which fluctuations have to be taken into account. Nevertheless, the only constant quantity during a RxMC simulation is the mass, and so it could appear interesting to compute also massic quantities.

C. Potential Model. All the simulations presented here have been performed with the program GIBBS, owned by IFP, Université Paris-Sud, and CNRS and developped in collaboration with CEA and other universities.[32]

The potential models used in this study to represent the NO_2 and N_2O_4 molecules have been basically optimized to reproduce phase diagram of the NO_2/N_2O_4 system at chemical equilibrium. Molecules have been considered as rigid bodies, and parameters are listed in Table 1. Concerning NO_2 molecule, the intramolecular distance d_{NO} and angle θ_{ONO} have been taken equal to equilibrium distance and angle from the COMPASS force field.[33] Atomic charges have also been taken from this force field and correctly reproduce the dipole moment of the isolated molecule (0.316 D). The N_2O_4 molecule is supposed to be planar; intramolecular geometry has been taken from the work of Kato et al.,[34] and atomic charges have been obtained through a Gaussian calculation using the B3LYP functionnal and the 6-31G* basis set. Finally, N−N and O−O dispersion−repulsion interactions have been modeled by a 6-12 Lennard-Jones (LJ) potential fitted to reproduce the phase equilibrium experimental data (liquid−vapor densities and mole fractions) of the N_2O_4/NO_2 system obtained by Reamer and Sage.[14] N−O LJ parameters have been obtained using Lorentz−Berthelot combining rules. Those parameters have been fitted to reproduce experimental data of the N_2O_4/NO_2 mixture at chemical equilibrium since pure N_2O_4, and pure NO_2 fluid properties do not exist experimentally. Furthermore, note that as partial charges have been determined first, LJ parameters implicitly include polarizability effects. Finally, this model appears more simple than the orientation-sensitive pairwise potential from Kato and co-workers[35] and does reproduce the chemical equilibrium (see section III for calculation results).

TABLE 1: Parameters Used to Model NO_2 and N_2O_4 Molecules

Geometry		
	NO_2	
d_{NO}	1.193 Å	ref 33
θ_{ONO}	134.1°	
q_N	0.146 e	
q_O	−0.073 e	
N_2O_4		
d_{NO}	1.19 Å	ref 34
d_{NN}	1.782 Å	ref 34
θ_{ONO}	135.4°	ref 34
q_N	0.588 e	
q_O	−0.294 e	
LJ Parameters		
σ_N	3.24 Å	
σ_O	2.93 Å	
ε_N/k	50.36 K	
ε_O/k	62.51 K	

The standard free enthalpy of the reaction $2NO_2 \rightleftarrows N_2O_4$ needed to obtain the acceptance probability of reaction move has been calculated from the free enthalpies of formation of NO_2 and N_2O_4 taken from the JANAF tables.[36]

The potential model used to represent the CO_2 molecule is the rigid version (EPM2) of the force field proposed by Harris and Yung.[37] Parameters are shown in Table 2. Note that Harris and Yung have developped their model using geometric combining rules for LJ sigma and epsilon. Nevertheless, in this work LJ parameters for the unlike interactions have been obtained using Lorentz−Berthelot rules. The use of an arithmetic combining rule for the calculation of sigma instead of a geometric rule is not expected to have a significant impact on the simulation results since O and C atoms do not exhibit a substantial size difference ($\sigma_O = 3.033$ Å and $\sigma_C = 2.757$ Å). The use of an arithmetic combining rule leads to a cross diameter σ_{CO} equals 2.895 Å, whereas a value of 2.892 Å is obtained with a geometric rule. Moreover, the paper of Nieto-Draghi and co-workers in 2007[38] shows that the combination of the Harris and Yung potential with the Lorentz−Berthelot rules allows a good restitution of both thermodynamic and transport properties of carbon dioxide.

In all simulations performed in this work, a cutoff for intermolecular interactions equal to the half of the simulation box length has been used to reduce the computing time. Beyond the cutoff, standard long-range corrections have been employed. Periodic boundary conditions have been added, and the reaction field method has been used to calculate long-range electrostatic interactions, except for simulations of pure CO_2 where a simple troncature has been used since quadrupole-quadrupole interactions decrease as $1/r^5$.

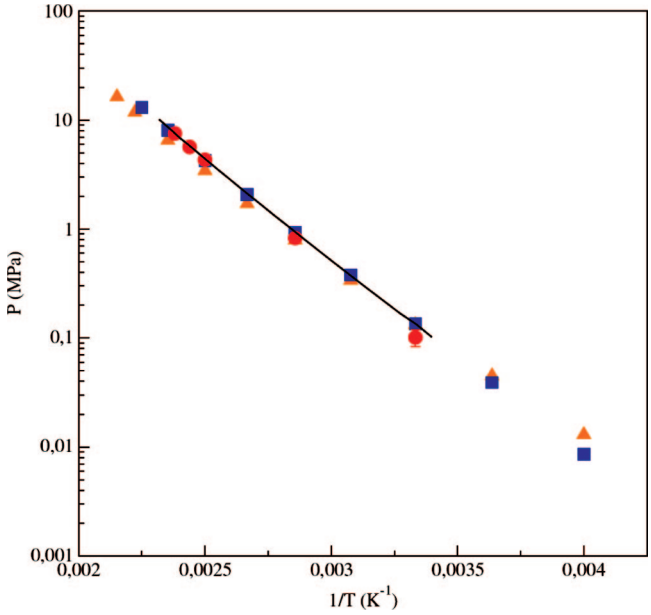

Figure 1. Inverse temperature dependence of pressure in the liquid−vapor coexistence region of the NO_2/N_2O_4 system, in logarithmic scale. The line represents the experiments of Reamer,[14] and our results are the red circles. The thermochemical modelizations of de Souza[17] are represented with the yellow triangles (HSA) and blue squares (SES).

TABLE 2: Parameters Used to Model CO_2 Molecules

	Geometry	
d_{CO}	1.149 Å	ref 37
θ_{OCO}	180.0°	
q_C	0.6512 e	
q_O	−0.3256 e	
	LJ Parameters	
σ_C	2.757 Å	ref 37
σ_O	3.033 Å	
ε_C/k	28.129 K	
ε_O/k	80.507 K	

The simulations concerning the NO_2/N_2O_4 system have been performed using the $N_{atoms}VT$ RxMC GEMC method. The system was initialized with between 200 and 300 molecules for each molecular specie. During those simulations, the respective probabilities of choosing a translation move, a rotation move, a volume change, a reaction move, and a transfer move were fixed at 0.4, 0.39, 0.01, 0.1, and 0.1. The convergence was generally obtained after 2×10^7 iterations, and averaging was performed on 5×10^7 iterations.

The simulations concerning the CO_2-NO_2/N_2O_4 system have been performed using the $N_{atoms}PT$ RxMC GEMC method. The system was again initialized with between 200 and 300 molecules for each molecular species. During those simulations, the respective probabilities of choosing a translation move, a rotation move, a volume change, a reaction move, and a transfer move were fixed at 0.3, 0.29, 0.01, 0.1, and 0.3. The convergence was generally obtained after 2×10^7 iterations, and averaging was performed on 10×10^7 iterations.

The number of locations and the number of orientations tested when inserting a molecule (k and k' parameters) have been set to 20. We chose to apply transfer moves to every type of molecules and to perform reaction moves in the two simulation boxes. Obviously, one could choose to apply transfer moves only to CO_2 and NO_2 and to perform reaction moves in the two boxes or to apply transfer moves to every type of molecules and to perform reaction moves only in the box representing the gas phase.

TABLE 3: Calculated Pressures (P), Mole Fractions of NO_2 ($x(NO_2)$), and Densities (ρ) of the Vapor (vap) and Liquid (liq) Phases in the Coexistence Region Using *NVT* RxMC GEMC Simulations and Our Potential Model

		vapor phase		liquid phase	
T (K)	P (MPa)	x_{vap} (NO_2)	ρ_{vap} (g·cm^{-3})	x_{liq} (NO_2)	ρ_{liq} (g·cm^{-3})
300	0.1012	0.349	3.14	0.002	1461
350	0.828	0.499	20.82	0.02	1330
400	4.322	0.584	104.4	0.117	1127
410	5.667	0.589	142.9	0.15	1083
420	7.537	0.583	198.9	0.2	1013

III. Results

A. NO_2/N_2O_4 System. In order to test the model developed for the NO_2/N_2O_4 system, we have performed five *NVT* RxMC GEMC simulations at five different temperatures between 300 and 420 K and computed the phase diagram of this reactive system. The results appear in Table 3 and Figures 1−3. Our results are compared on the one hand to experimental results from Reamer and Sage[14] and on the other hand to modelizations from de Souza and Deiters.[17] In their work, de Souza and Deiters have modeled the liquid−vapor equilibrium of this reacting system using two molecular-based equations of state involving hard spheres for repulsion and different expressions with adjustable parameters for attraction.

With the model we have developped, the temperature dependence of pressure in the liquid−vapor coexistence region is well described. At high temperature, our Monte Carlo results appear closer to the experimental values than both modelisations of de Souza, the HSA model (hard sphere with an attractive mean field component) and the SES model (semi-empirical equation of state). Small discrepancies appear at lower pressure. This is due to the difficulty to evaluate the pressure using statistical method when the pressure is too low. As a consequence, an important statistical uncertainty is associated to these values.

The temperature dependence of liquid and vapor densities at equilibrium is also well described by our model, although it slightly overestimates the liquid density, particularly in the critical region. The critical point has been evaluated by fitting the liquid and vapor densities to the rectilinear diameter rule and to the scaling relationship for the width of the coexistence curve:

$$\frac{\rho_{liq} + \rho_{vap}}{2} = \rho_c + A(T - T_c) \qquad (3.18)$$

$$\rho_{liq} - \rho_{vap} = B(T - T_c)^{\beta} \qquad (3.19)$$

where β is the critical exponent, taken to be equal to 0.325. The critical point we have obtained ($\rho_c = 577$ g·cm^{-3}; $T_c = 441$ K) appears closer to the experimental one (550 g·cm^{-3}; 431.4 K) than the ones obtained by de Souza et al.[17] Indeed, the HSA model gives a good critical density but overestimates the temperature (541 g·cm^{-3}; 465 K), and on the contrary, the HSA model gives a good temperature but overestimates the density (611 g·cm^{-3}; 444 K).

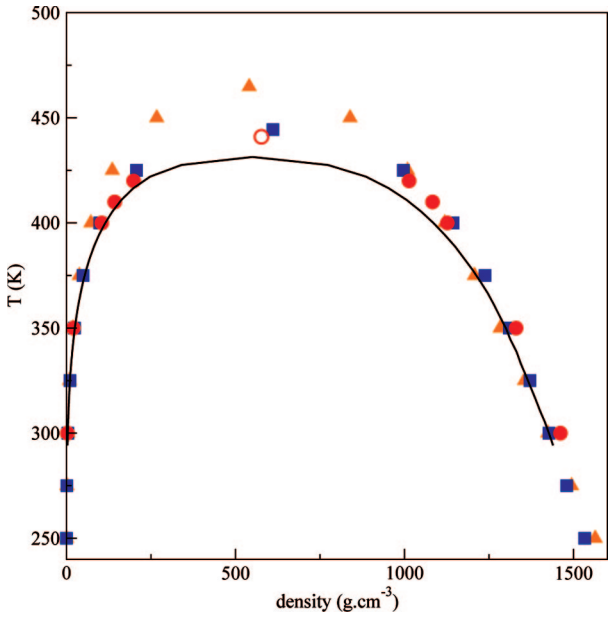

Figure 2. Temperature dependence of density in the liquid−vapor coexistence region of the NO_2/N_2O_4 system. The line represents the experiments of Reamer,[14] and our results are the red circles (the open circle is the critical point). The thermochemical modelizations of de Souza[17] are represented with the yellow triangles (HSA) and blue squares (SES).

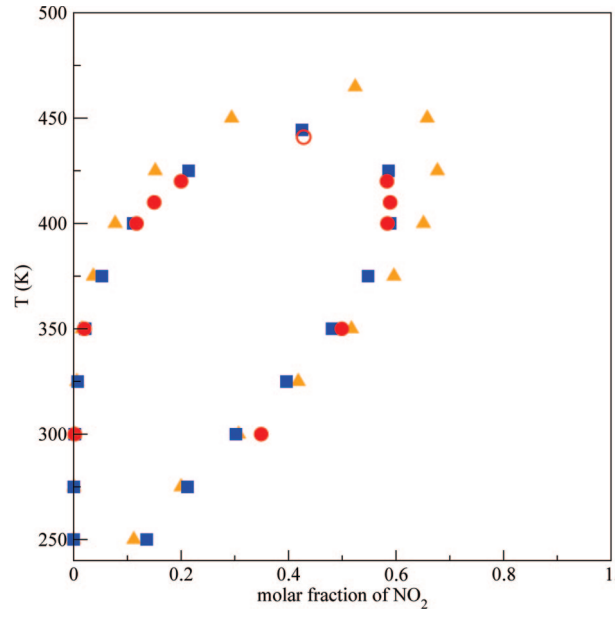

Figure 3. Temperature dependence of the mole fraction of NO_2 in the liquid−vapor coexistence region of the NO_2/N_2O_4 system. Our results are represented with the red circles and the thermochemical modelisations of de Souza[17] are represented with the yellow triangles (HSA) and blue squares (SES).

Finally, using our model, we obtain a temperature dependence of the mole fraction of NO_2 in the mixture at equilibrium equivalent to the one obtained by de Souza using the semi-empirical equation of state model.[17] This SES model was found to give more accurate results than the HSA approach in the work of de Souza. Those results allow us to affirm that our model is well adapted to describe the NO_2/N_2O_4 mixture at chemical equilibrium.

The last part of this study on the NO_2/N_2O_4 reacting system concerns monophasic simulations in the reaction ensemble at constant pressure and temperature combined with derivative properties calculations. Equations 2.8 and 2.10−2.15 described above have been used to compute isobaric heat capacities at 0.01 and 0.1 MPa for temperatures in the range 250 to 500 K. Calculated heat capacities are compared to experimental data of McCollum at 0.1 MPa.[18] Results are given in Table 4 and illustrated in Figure 4a.

The heat capacity of such a reacting mixture is composed of three contributions: the contribution of dinitrogen tetroxide molecules, the contribution of nitrogen dioxide molecules, and the heat associated to the dissociation of dinitrogen tetroxide in nitrogen dioxide as the temperature is raised. This third contribution exists only in the temperature range where dissociation occurs. As the dissociation of N_2O_4 is an endothermic reaction ($\Delta_r H° = 13.67$ kcal·mol^{-1} at 298.15 K), more NO_2 in the mixture means more energy being absorbed, thus a positive contribution appears in the heat capacities profile as shown in Figure 4a. An analysis of the shape of such isobaric heat capacity curves in the case of reacting mixtures can be found in the work of Braibanti et al.,[39] showing convexity (respectively concavity) for endothermic (respectively exothermic) reactions in comparison with non reacting mixtures. Ideal heat capacities of pure NO_2 and pure N_2O_4, taken from the JANAF tables, are also reported in Figure 4a in the temperature range 200−500 K. These ideal gas values have been proposed by Chase using statistical mechanical calculations described in ref 36 from the knowledge of principal moments of inertia, symmetry number, vibrational frequencies, and electronic levels of the studied molecule. These NO_2 and N_2O_4 pure component properties have been extrapolated into temperature regions where the pure

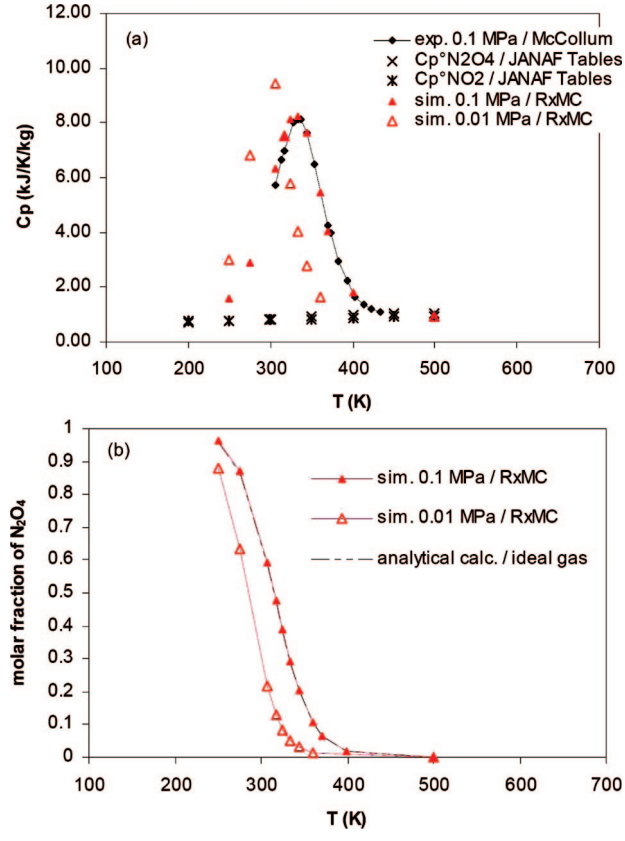

Figure 4. (a) Temperature and pressure dependence of heat capacities at 0.1 MPa of the NO_2/N_2O_4 equilibrium mixture. Results obtained from Monte Carlo simulations in the reaction ensemble (triangles) are compared to experimental data of McCollum[18] at 0.1 MPa (diamonds). (b) Temperature and pressure dependence of equilibrium compositions of the NO_2/N_2O_4 mixture.

TABLE 4: Calculated Heat Capacities at Constant Pressure (0.01 and 0.1 MPa) for the NO_2/N_2O_4 System Using RxMC Simulations[a]

	C_P (kJ·kg^{-1}·K^{-1})		
	exp (McCollum[18])	sim (RxMC, this work)	
T (K)	0.1 MPa	0.01 MPa	0.1 MPa
250.		3.00	1.56
275.		6.83	2.87
306.88	5.73	9.43	6.34
314.15	6.64		
317.15	7.01	7.51	7.55
325.		5.78	8.15
328.18	8.01		
334.05	8.10	4.04	8.26
336.48	8.15		
343.85	7.65	2.76	7.62
354.04	6.51		
360.		1.64	5.44
370.66	4.23		4.03
373.15	3.98		
383.15	2.96		
393.15	2.24		
400.	-		1.80
403.15	1.63		
413.15	1.37		
423.15	1.20		
433.15	1.10		
500.		0.94	0.96

[a] Comparison with experimental data of McCollum[18] at 0.1 MPa.

component is not necessarily the most stable specie. In the present study, these ideal gas values have been used to account for the contributions to the total heat capacity of both the kinetic energy and the internal potential energy that are not considered in our Monte Carlo simulations.

Good agreement is obtained between simulation results and experimental data at 0.1 MPa. Comparison between results obtained at 0.01 and 0.1 MPa illustrates the pressure dependence of the heat capacity. This observed dependence, even at such low pressures, is due to the pressure dependence of the equilibrium mixture composition. These equilibrium mixture compositions are shown in Figure 4b, along with the composition derived from analytical calculations based on ideal-gas assumption. As expected, simulation results at 0.1 MPa are identical to ideal-gas calculations and a low pressure favors the formation of monomers NO_2 in the mixture.

B. CO_2-NO_2/N_2O_4 System. Calculations of the liquid−vapor equilibrium properties of the CO_2-NO_2/N_2O_4 mixture have been performed using combined RxMC and GEMC simulations. Unlike macroscopic equation of state approaches, no calibration on experimental information concerning the mixture is required to perform these predictive calculations. The only required data are the previously described pure component liquid−vapor properties, as well as ideal gas data. Phase diagrams have been calculated at three different temperatures: 300, 313, and 330 K. The only experimental data available for this mixture are the ones reported by Belkadi.[4] Calculated phase envelopes are shown in Figure 5a−c. Numerical values are given in Table 5. In the different graphs of Figure 5, triangles represent our Monte Carlo simulation results, while the open circles correspond to the experimental data. Full lines represent the results obtained by Belkadi and co-workers[4] using the crossover soft-SAFT equation of state with a binary interaction parameter calibrated on the available experimental isotherm at 313 K. The lowest studied temperature, 300 K, is just below the critical temperature of CO_2, explaining why the phase diagram ends up at the vapor pressure of pure CO_2 at this imposed temperature. The two other studied temperatures are above the critical temperature of CO_2; hence, the corresponding phase diagrams display a liquid−vapor critical point. The critical coordinates P_c, ρ_c, and w_c (critical pressure, critical density, and critical weight composition) have been determined using some extrapolations based on the following scaling laws:[32]

$$\rho_i = \rho_c + \epsilon\frac{\gamma}{2}(P_c - P)^{\beta} + \lambda(P_c - P) \qquad (3.20)$$

$$w_i = w_c + \left(\lambda_1 - \epsilon\frac{\lambda_2}{2}\right)(P_c - P) - \epsilon\frac{\mu}{2}(P_c - P)^{\beta} \qquad (3.21)$$

where $\epsilon = 1$ for the liquid phase and $\epsilon = -1$ for the vapor phase. The critical coordinates (P_c, ρ_c, and w_c) as well as the five parameters (γ, λ, λ_1, λ_2, μ) involved in expressions 3.20 and 3.21 are regressed from a set of coexistence points (P, ρ_l, ρ_v) and (P, w_l, w_v) below the critical point. Critical coordinates obtained using this procedure are: $P_c = 7.79$ MPa, $\rho_c = 554$ g·cm^{-3}, and $w_c(CO_2) = 0.87$ at 313 K and $P_c = 9.36$ MPa, $\rho_c = 584$ g·cm^{-3}, and $w_c(CO_2) = 0.79$ at 330 K.

Our predictions show good agreement with the empirical modeling results of Belkadi.[4] Reasonable quantitative agreement is also observed between our predictions and the experimental data at 313 K, although a slight overestimate of the calculated bubble pressures is observed. This overestimate could be mainly attributed to the force field used to model CO_2 molecules. Indeed, as shown in Figure 6, the EPM2 potential of Harris and Yung tends to overestimate the saturation pressure of CO_2 by more than 10%.

Compositional and volumetric information on the coexisting phases can also be derived from our Monte Carlo simulations of the CO_2-NO_2/N_2O_4 mixture. The coexisting densities calculated at 300 K are shown in Figure 7. Concerning the molar compositions of coexisting phases, our simulations at 300 K predict very low amount of non associated NO_2 molecules in both phases. No experimental or modeling results are available in the literature to allow comparisons with our predictions.

Derivative properties of the CO_2-NO_2/N_2O_4 mixture have been calculated using the fluctuation method in the isothermal−isobaric reaction ensemble. These calculations have been performed at 1 MPa and imposed temperatures in the range 250−400 K. The mixture investigated is composed of 80 wt% CO_2 and 20 wt% NO_2/N_2O_4. This composition was selected because it is representative of a CO_2 stream of very low quality, certainly worse than what could be encountered in carbon dioxide capture and storage operations. The objectives of such calculations are to address the impact of a few percent of NO_2/N_2O_4 contaminants on the thermophysical properties of the CO_2 stream. Calculated heat capacities of this CO_2-NO_2/N_2O_4 mixture are compared to pure CO_2 heat capacities. Results are presented in Figure 8. For pure CO_2, comparison is made between calculated values at three different pressures and the IUPAC recommended data.[40] Good agreement is observed. Results obtained at 1 MPa for pure CO_2 show that simulation correctly represents the difference between heat capacities in the gas and liquid states. At 10 MPa, i.e. at a pressure not too far from the critical pressure of CO_2 (7.38 MPa), simulation manages to reproduce qualitatively the increase of the isobaric heat capacity as the temperature goes close to the critical

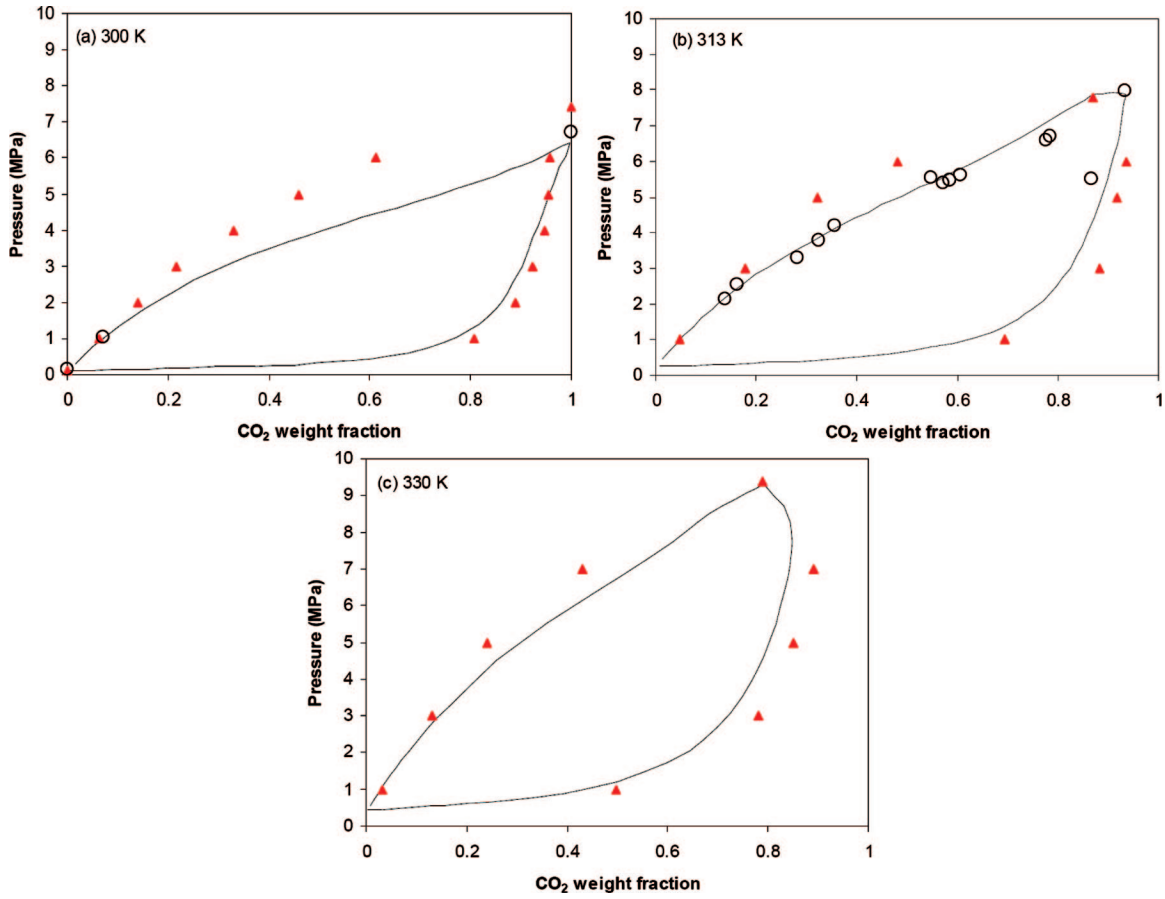

Figure 5. Pressure−composition diagram of the CO_2−NO_2/N_2O_4 mixture at three different temperatures: 300 (a), 313 (b), and 330 K (c). Triangles are Monte Carlo simulation results. The associated statistical uncertainties are in most cases smaller than the symbol size. Full lines represent the results obtained by Belkadi and co-workers[4] using the crossover soft-SAFT equation of state. Open circles are experimental data taken from the paper of Belkadi or from the NIST webbook for pure component vapor pressures.[41]

TABLE 5: Simulation Results of the Liquid−Vapor Equilibrium of the CO_2−NO_2/N_2O_4 Mixture[a]

T (K)	P (MPa)	ρ_l (kg·m^{-3})	ρ_v (kg·m^{-3})	$w_l(CO_2)$	$w_v(CO_2)$
300	1.0	1422.8	20.4	0.063	0.808
	2.0	1380.7	41.4	0.139	0.890
	3.0	1334.1	65.0	0.217	0.923
	4.0	1266.1	92.4	0.329	0.946
	5.0	1180.4	126.0	0.460	0.954
	6.0	1079.0	180.0	0.613	0.957
313	1.0	1405.5	20.5	0.047	0.695
	3.0	1322.0	62.1	0.178	0.882
	5.0	1233.0	117.1	0.322	0.917
	6.0	1114.6	148.8	0.481	0.937
330	1.0	1375.6	21.1	0.033	0.497
	3.0	1309.7	60.7	0.130	0.778
	5.0	1227.2	108.1	0.241	0.851
	7.0	1087.6	170.7	0.428	0.892

[a] Liquid and vapor densities ρ_l and ρ_v are in kilograms per cubic meter; $w_l(CO_2)$ and $w_v(CO_2)$ are the CO_2 weight fractions in the liquid and vapor phases.

temperature of CO_2 (304.2 K). At higher pressure (50 MPa), simulation accurately reproduces the slight decrease of the total heat capacity with increasing temperature, which is due to a decrease of the residual heat capacity which overweights the increase in ideal heat capacity. These results confirm the capability of molecular simulations to predict properties which were not taken into account in the optimization of the intermolecular potential, as it was the case for the CO_2 Harris and Yung potential which was optimized only on liquid−vapor properties.

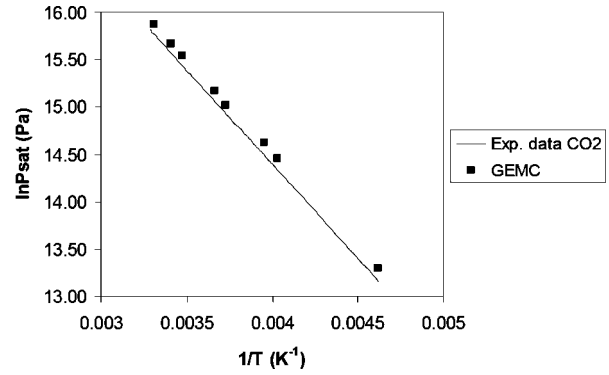

Figure 6. Comparison between Gibbs ensemble simulation results obtained with the EPM2 potential[37] and experimental vapor pressures[41] for CO_2.

For the CO_2 + NO_2/N_2O_4 mixture, calculated heat capacities at 1 MPa are systematically higher than the obtained values for pure CO_2. For thermodynamic conditions where nitrogen oxides exist as a mixture of monomers and dimers, an increase of more than 50% of the total heat capacity can be observed when NO_2/N_2O_4 are added in gaseous CO_2. As discussed above, this effect is due to the endothermic dissociation of N_2O_4 molecules as the temperature is increased. Such calculations show the importance of accounting for the reactivity of the system since it will impact the amount of heat that must be provided to the fluid to raise its temperature and thus influence the energy cost of an industrial operation.

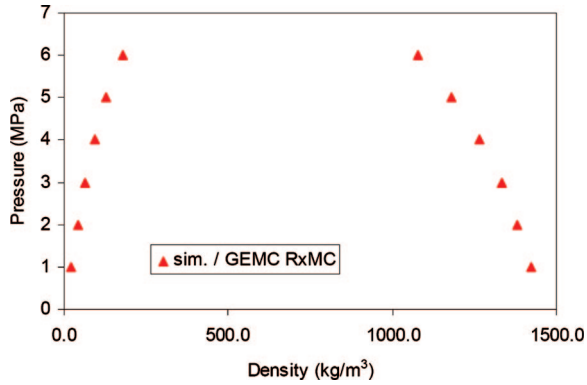

Figure 7. Coexisting densities of the CO_2-NO_2/N_2O_4 system at 300 K.

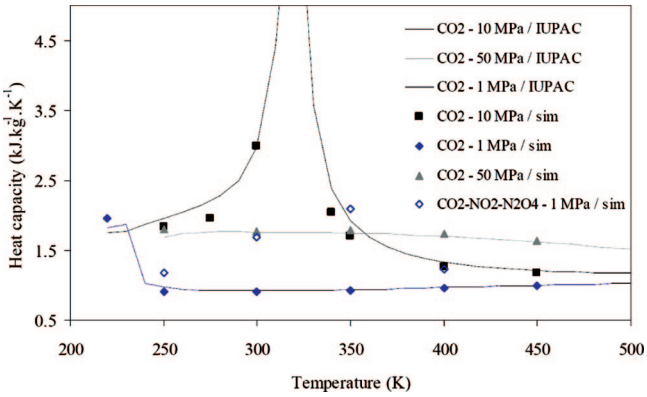

Figure 8. Isobaric heat capacities of pure CO_2 (filled symbols) and $CO_2 + 20$ wt% NO_2/N_2O_4 (open symbols) calculated using isothermal−isobaric Monte Carlo simulations at different pressure and temperature conditions. The full lines represent the IUPAC recommended values for pure CO_2.

IV. Conclusion

The combined use of GEMC and RxMC simulations has proved to be a powerful tool to study the equilibrium properties of a multiphase system including chemical reactions. In the present study, this technique has been used to predict the thermodynamic behavior of the $CO_2 + NO_2/N_2O_4$ system, without any parametrization on the mixture properties. The only adjustable parameters used in this study are the parameters of the pure component intermolecular potentials used for CO_2 and NO_2/N_2O_4 molecules. In the case of NO_2 and N_2O_4 molecules, accurate potential parameters have been proposed that allow good restitution of the liquid−vapor properties of the reacting system. The $CO_2 + NO_2/N_2O_4$ phase diagrams calculated at different temperatures show good agreement both with experimental data and with equation of state modeling results available in the literature.[4] Information about the ratio of associated and nonassociated nitrogen oxide molecules in the coexisting phases has also been given. Such information, that is straightforward using molecular simulation, is often difficult to access experimentally. In addition to these liquid−vapor equilibrium properties, some derivative properties have also been calculated for both NO_2/N_2O_4 and $CO_2 + NO_2/N_2O_4$ systems. These calculations, performed in the reaction ensemble, have used fluctuation formula that account for energy fluctuations together with fluctuations of number of molecules and composition. The calculated heat capacities show a maximum in the temperature range where N_2O_4 dissociation occurs, in agreement with available experimental data. Such calculations confirm the capability of molecular simulation to predict properties which were not taken into account in the optimization procedure of the intermolecular potentials.

This work shows that molecular simulation can play a significant role in some industrial applications. In the context of carbon dioxide capture and storage operations, molecular simulation can be of help to study the thermodynamic properties of CO_2 and CO_2−contaminant mixtures under a large range of pressure, temperature, and compositional conditions. This technique does no longer require expensive computational resources and has now reached an intermediate position between experimental measurements and thermodynamic models based on equations of state. Work is now under progress to study the thermodynamic behavior of some more complex mixtures including different contaminants and several chemical reactions.

Acknowledgment. Financial support from the French Agence Nationale de la Recherche (ANR-07-BLAN-0268) is gratefully acknowledged.

References and Notes

(1) IPCC. *Special report on carbon dioxide capture and storage*; Technical report, Cambridge University Press: New York,. 2005.
(2) I.G.G.R. Programme *Impact of impurities on CO_2 capture, transport and storage*, Report PH4/32, **2004**.
(3) Anheden, M.; Andersson, A.; Bernstone, C.; Eriksson, S.; Yan, J.; Liljemark, S.; Wall, C. In *Proceedings of the GHGT 7 Conference*, CO_2 Quality Requirement for a System with CO_2 Capture, Transport and Storage, Vancouver, Canada, Sept 5−9, 2004.
(4) Belkadi, A.; Llovell, F.; Gerbaud, V.; Vega, L. *Fluid Phase Eq.* **2008**, *266*, 154–163.
(5) Pastirk, I.; Comstock, M.; Dantus, M. *Chem. Phys. Lett.* **2001**, *349*, 71–78.
(6) Yoshino, K.; Esmond, J.; Parkinson, W. *Chem. Phys.* **1997**, *221*, 169–174.
(7) Verhoek, F.; Daniels, F. *J. Am. Chem. Soc.* **1931**, *53*, 1250–1263.
(8) Harris, L.; Churrey, K. *J. Chem. Phys.* **1967**, *47*, 1703–1709.
(9) Cher, M. *J. Chem. Phys.* **1962**, *37*, 2564–2570.
(10) James, D.; Marshall, R. *J. Phys. Chem.* **1968**, *72*, 2963–2966.
(11) Chao, J.; Wilhoit, R.; Zwolinski, B. *Thermochim. Acta* **1974**, *10*, 359–371.
(12) Kato, T. *J. Chem. Phys.* **1996**, *105*, 4511–4521.
(13) Ornellas, F.; Resende, S.; Machado, F.; Roberto-Neto, O. *J. Chem. Phys.* **2003**, *118*, 4060–065.
(14) Reamer, H.; Sage, B. *Ind. Eng. Chem.* **1952**, *44*, 185–187.
(15) Gray, P.; Rathbone, P. *J. Chem. Soc.* **1958**, 3550–3557.
(16) Giauque, W.; Kemp, J. *J. Chem. Phys.* **1938**, *6*, 40–52.
(17) de Souza, L.; Deiters, U. *Phys. Chem. Chem. Phys.* **2000**, *2*, 5606–5613.
(18) McCollum, E. *J. Am. Chem. Soc.* **1927**, *49*, 28–38.
(19) Smith, W.; Triska, B. *J. Chem. Phys.* **1994**, *100*, 3019.
(20) Johnson, J.; Panagiotopoulos, A.; Gubbins, K. *Mol. Phys.* **1994**, *81* (3), 717.
(21) Turner, C.; Brenan, J.; Smith, M.; Lisal., W.; Johnson, J.; Gubbins, K. *Mol. Sim.* **2008**, *34*, 119–146.
(22) Panagiotopoulos, A. *Mol. Phys.* **1987**, *61*, 813–826.
(23) Lísal, M.; Nezbeda, I.; Smith, W. R. *J. Chem. Phys.* **1999**, *110* (17), 8597–8604.
(24) Lísal, M.; Smith, W. R.; Nezbeda, I. *AIChE J.* **2000**, *46*, 866–875.
(25) Johnson, J. *Adv. Chem. Phys.* **1999**, *105*, 461.
(26) Bourasseau, E.; Dubois, V.; Desbiens, N.; Maillet, J.-B. *J. Chem. Phys.* **2007**, *127*, 084513.
(27) Hervouet, A.; Desbiens, N.; Bourasseau, E.; Maillet, J.-B. *J. Phys. Chem. B* **2008**, *112*, 5070.
(28) Shaw, M. *J. Chem. Phys.* **1991**, *94*, 7550.
(29) Shaw, M. In *Proceedings of the AIP conference Shock Compression and Condensed Matter*, A Hybrid Monte Carlo Method for Equilibrium Equation of State of Detonation Products, Atlanta, June 24−29, 2001.
(30) Bourasseau, E.; Ungerer, P.; Boutin, A. *J. Phys. Chem. B* **2002**, *106*, 5483.
(31) Lagache, M.; Ungerer, P.; Boutin, A.; Fuchs, A. *Phys. Chem. Chem. Phys.* **2001**, *3*, 4333–4339.
(32) Ungerer, P.; Tavitian, B.; Boutin, A. *Applications of Molecular Simulation in the Oil and Gas Industry*; IFP Publications, Paris, 2005.
(33) Yang, J.; Ren, Y.; Tian, A. *J. Chem. Phys. B* **2000**, *104*, 4951–4957.
(34) Kato, T.; Oobatake, M.; Machida, K.; Hayashi, S. *Mol. Phys.* **1992**, *77* (1), 177–192.

(35) Kato, T.; Hayashi, S.; Machida, K. *J. Chem. Phys.* **2001**, *115*, 10852–10862.
(36) Chase, M. W. *NIST−JANAF Thermochemical Tables*, 4th ed.; Monograph No. 9; American Institute of Physics: College Park, MD, 1998.
(37) Harris, J.; Yung, K. *J. Phys. Chem.* **1995**, *99*, 12021–12024.
(38) Nieto-Draghi, C.; de Bruin, T.; Perez-Pellitero, J.; Bonet Avalos, J.; Mackie, A. D. *J. Chem. Phys.* **2007**, *126*, 064509.
(39) Braibanti, A.; Fisicaro, E.; Compari, C. *Phys. Chem. Chem. Phys.* **2000**, *2*, 4870–4875.
(40) Angus, S.; Armstrong, B.; de Reuck, K. M. *IUPAC, Carbon Dioxide, International Thermodynamic Tables of the Fluid State*; Pergamon Press: Elmsford, NY, 1976.
(41) Data taken from The Saturation Properties of Carbon Dioxide. http://webbook.nist.gov (accessed June, 2006).

JP8068255